Revisiting the Agung 1963 volcanic forcing — impact of one or two eruptions

Ulrike Niemeier[1], Claudia Timmreck[1], and Kirstin Krüger[2]

[1]Max Planck Institute for Meteorology, Bundesstr. 53, 20146 Hamburg, Germany
[2]Department of Geosciences, University of Oslo, Blindern, 0315 Oslo, Norway

Correspondence: U. Niemeier (ulrike.niemeier@mpimet.mpg.de)

Abstract. In 1963 a series of eruptions of Mt. Agung, Indonesia, resulted in the 3rd largest eruption of the 20th century and claimed about 1900 lives. Two eruptions of this series injected SO_2 into the stratosphere, a requirement to get a long lasting stratospheric sulfate layer. The estimated mass flux of the first eruption was about twice as large as the mass flux of the second eruption. We followed the estimated emission profiles and assumed for the first eruption on March 17th an injection rate of 4.7
Tg SO_2, and 2.3 Tg SO_2 for the second eruption on May 16th. The injected sulfur forms a sulfate layer in the stratosphere. The evolution of sulfur is non-linear and depends on the injection rate and aerosol background conditions. We performed ensembles of two model experiments, one with a single and a second one with two eruptions. The two smaller eruptions result in a lower burden, smaller particles and 0.1 to 0.3 Wm^{-2} (10 - 20%) lower radiative forcing in monthly mean global average compared to the individual eruption experiment. The differences are the consequence of slightly stronger meridional transport due to different seasons of the eruptions, lower injection height of the second eruption and the resulting different aerosol evolution.

Overall, the evolution of the volcanic clouds is different in case of two eruptions than with a single eruption only. The differences between the two experiments are significant. We conclude that there is no justification to use one eruption only and both climatic eruptions should be taken into account in future emission datasets.

1 Introduction

In September 2017 Mt. Agung, a volcano on Bali, Indonesia (8.342°S, 115.58°E), became restless. Earthquakes, steam, ash clouds and lahars resulted in the evacuation of nearly 150.000 people from the volcano's environment within a radius of 9-12 km in November 2017 (Gertisser et al., 2018). The eruption resulted in an ash cloud reaching up to an altitude of about 9.3 km (Marchese et al., 2018) and about 10 DU SO_2 above Bali (Hansen, 2017), which was not large and high enough to result in a climatic impact. The last climatic eruption of Mt. Agung dates back more than 50 years. From February 1963 to January 1964 a series of eruptions from Mt. Agung are documented (Fontijn et al., 2015). The initial unrest resulted in the 3rd largest eruption of the 20th century global volcano record and claimed about 1900 lives. Revising the literature, it is obvious that not just one of the eruptions was strong enough to inject SO_2 into the stratosphere, a requirement to get a long lasting stratospheric sulfate layer, but also a second one (Self and Rampino, 2012). The mass flux of the second eruption on March 16th was about half the size of the mass flux of the first eruption on March 17th. Self and Rampino (2012) estimate the volumetric eruption

rate for March 17th to be $\sim 1.8 \times 10^4$ m^{3}s^{-1} over ~ 3.5 h duration. The volumetric eruption rate of the May 16th event was $\sim 0.9 \times 10^4$ m^{3}s^{-1} over ~ 4 h duration. The resulting sulfate layer caused a climatic impact by scattering and absorbing solar and terrestrial radiation leading to a temperature decrease of about 0.4 K in the tropical troposphere (Hansen et al., 1978).

The sulfate load of the Mt. Agung eruptions was estimated to $7 - 7.5$ Tg SO$_2$ from observations of aerosol optical depth (AOD) a couple of months after the eruption (Self and King, 1996). It was impossible to distinguish between single eruptions with this method. This could be the reason, that up to now, recent volcanic forcing data sets assume one large eruption phase of 7 Tg SO$_2$ for Mt. Agung, the one in March 1963, but neglect the second one. Within this paper we examine whether or not it is important to consider both eruption phases individually when simulating sulfate evolution and transport, as well as the impact on radiative forcing of the Mt. Agung eruption.

The radiative forcing of the sulfate aerosols can either be simulated by calculating the evolution and transport of sulfur with an aerosol microphysical model or, much simpler, by prescribing the optical parameters of the volcanic aerosols. The first needs volcanic injection data and information on emission strength and altitude, the latter optical properties like the aerosol optical depth (AOD). Most datasets base the estimated global coverage of sulfate aerosols after the Mt. Agung eruption on ground based and on ice core measurements, and provide the AOD (e.g. Sato et al. (1993), Stenchikov et al. (1998), Ammann et al. (2003), Crowley et al. (2008), Crowley and Unterman (2012)). Satellite data were yet not available in 1963. Newer datasets rely not only on measurements, but they also include simulated sulfate distributions, e.g. results of an empirical aerosol forcing generator like Easy Volcanic Aerosol (EVA) (Toohey et al., 2016) or complex aerosol models, which simulate the evolution of the aerosol e.g. Arfeuille et al. (2014) for the SAGE-4λ data set. On the other hand new volcanic eruption data sets are released which provide the SO$_2$ injection rate for large climate relevant volcanic eruptions, e.g. Volcanic Emissions for Earth System Models (VolcanEESM) (Neely III and Schmidt, 2016) and the eVolv2k data set (Toohey and Sigl, 2017), provide sulfur injection data. These newer datasets include one eruption phase only for Mt. Agung, the main eruption in March 1963, and assume the injected amount of SO$_2$ of 7 Tg following the estimates of Self and King (1996).

The evolution of the volcanic aerosols is strongly non-linear. In particular, the particle size depends on the erupted mass (Timmreck et al. (2010), Niemeier and Timmreck (2015)) and sulfur injected into an existing volcanic sulfate layer evolves differently than sulfur injected into background conditions (Laakso et al., 2016). Additionally, many chemical processes depend on particle size and sulfate concentrations. For example stratospheric OH, NO$_x$ and ozone concentrations change under high sulfur load. CCMVal (2010) shows in Figure 8.20 the temperature response of different stratospheric chemistry models to volcanic sulfate aerosols. Models using full aerosol microphysics or prescribing surface aerosol density tend to overestimate the measured heating in the stratosphere after the Mt. Agung eruption. This might be related to the assumption of one eruption phase only, especially as for the Mt. Pinatubo eruption in 1991 the models show a slightly better result.

In this study we would like to address the following question: Is there a significant difference when simulating two medium eruptions instead of a single large one? We performed two experiments to provide an answer to this question. We describe the model and the simulations in more details in Section 2, show results in Section 3 where we describe the different burden results of the two experiment ensembles (Sect. 3.1) and the cumulative impact of the eruptions (Sect. 3.2). Finally, we compare our results to measurements in Section 4 before we are concluding in Section 5.

2 Model and observation data

2.1 Model setup

The model simulations of this study were performed with the middle atmosphere version of the general circulation model (GCM) MAECHAM5 (Giorgetta et al., 2006). The aerosol microphysical model HAM (Stier et al., 2005) is interactively
5 coupled to the GCM and was extended to a stratospheric version (Niemeier et al., 2009). MAECHAM5-HAM, ECHAM-HAM later in the text, was applied with the spectral truncation at wave-number 42 (T42), a horizontal grid size of about $2.8°$, and 90 vertical layers (L90) up to $0.01\,\mathrm{hPa}$. The model is not coupled to an ocean model and shows pure volcanic forcing response only. The sea surface temperatures (SST) are set to monthly mean climatological values based on the Atmospheric Model Intercomparison Project (AMIP) SST observational data set (Hurrell et al., 2008). Thus, the SST does not reflect the historical
10 date but rather represents a climatological mean.

HAM calculates the evolution of sulfate from the injected SO_2 to sulfate aerosol, including nucleation, accumulation, condensation, and coagulation, as well as transport and sink processes like sedimentation and deposition (Stier et al., 2005). A simple stratospheric sulfur chemistry is applied above the tropopause (Timmreck, 2001; Hommel et al., 2011) and the sulfate is radiatively active. The model setup is described in more detail in Niemeier et al. (2009) and Niemeier and Schmidt (2017).
15 The L90 version of MAECHAM5-HAM generates interactively a quasi-biennial oscillation (QBO) (Giorgetta et al., 2006). However, we decided to nudge the QBO in the tropical stratosphere to the observed monthly mean winds at the Equator (updated Naujokat (1986)), as described in Giorgetta and Bengtsson (1999). This allows us to inject the volcanic sulfur into the observed QBO phase and still include the better resolved transport processes of the L90 version, e.g. a less permeable subtropical transport barrier (Niemeier and Schmidt, 2017). Nudging the QBO prescribes the feedbacks of the sulfate aerosol
20 heating in the stratosphere on the QBO winds as observed. However, the QBO winds are prescribed on a monthly basis. This may suppress very short term changes in the transport due to dynamical changes caused by aerosol heating at the equatorial stratosphere.

2.2 Model simulations

We performed experiments of two scenarios for the 1963 eruption of Mt. Agung. We assumed for the first experiment one
25 eruption phase at March 17th (AGUNG1) with an injection of $7\,\mathrm{Tg}\,SO_2$ over three hours. For the second scenario two eruptions were simulated with a ratio of the injection rate of 2:1. This reflects the ratio of the volumetric eruption rate and the mass flux of $4\,\mathrm{kg\,s^{-1}}$ and $2\,\mathrm{kg\,s^{-1}}$ given in Table 3 in Self and Rampino (2012). The altitudes of the eruptions were taken as average of the range of estimated altitudes in Self and Rampino (2012). This resulted for the second experiment in the following assumption of two eruptions phases (AGUNG2): The first on March, 17th over three hours and an injection rate of $4.7\,\mathrm{Tg}\,SO_2$ at an
30 altitude of $50\,\mathrm{hPa}$ and a second on May, 16th over four hours and an injection rate of $2.3\,\mathrm{Tg}\,SO_2$ at a slightly lower altitude of $70\,\mathrm{hPa}$. The ECHAM5-HAM input data for the eruptions are summarized in Table 1.

We performed a set of six ensemble members for each eruption case. See supplementary material for further details. All six simulations were used to calculate an ensemble mean. Additionally, we performed a single simulation were an eruption altitude of 50 hPa was assumed for both eruptions (AGUNG2-50hPa).

Table 1. Overview over the performed simulations and information to the eruption details, after (Self and Rampino, 2012).

| Simulation name	Eruption mass	Eruption altitude	Eruption duration	Eruption date	Ensemble members	OH-limitation
AGUNG1	7 Tg SO_2	50 hPa	6 - 9 UTC	March 17th 1963	6	no
AGUNG2	4.7 Tg SO_2	50 hPa	6 - 9 UTC	March 17th 1963	6	no
	2.3 Tg SO_2	70 hPa	17 - 21 UTC	May 16th 1963		
AGUNG2 50 hPa	4.7 Tg SO_2	50 hPa	6 - 9 UTC	March 17th 1963	1	no
	2.3 Tg SO_2	50 hPa	17 - 21 UTC	May 16th 1963		

2.3 Observations

5 We compare our simulation results to observations and volcanic data sets provided for the climate model intercomparison project (CMIP). The AOD prescribed for the years 1963 to 1964 in the CMIP5 simulations of the Max Planck Institute for Meteorology is based on Sato et al. (1993) and Stenchikov et al. (1998). The data rely mainly on astronomical observations summarized by Dyer and Hicks (1968), as no satellite data are available for the period. The AOD data for CMIP6 were taken from the SAGE-3λ database (Luo (2016), Revell et al. (2017)). They combine ice core data (Gao et al., 2008) and AOD data 10 (Stothers, 2001) with aerosol microphysical model simulations and include only one eruption of Mt. Agung in their preparatory model simulations (Arfeuille et al., 2014).

Stothers (2001) assembled a revised chronology of observed AOD after the Mt. Agung eruption. The data contain mainly measurements of atmospheric attenuation of starlight and direct sunlight. Stothers (2001) provides values of monthly mean AOD data as an average over different measurement sites, between 20°N to 40°N and 20°S to 40°S and results of monthly 15 mean data of single measurement sites. Stothers (2001) excluded data of tropical measurement sites because they were not reliable.

Radiosonde temperature measurements provide information on the heating of the stratospheric aerosol layer after the eruption. This heating causes changes in stratospheric dynamics (Aquila et al. (2014), Toohey et al. (2013)) and is, therefore, an important value which should be taken into account correctly. Free and Lanzante (2009) provide vertical temperature anoma-20 lies after volcanic eruptions from radiosonde data (RATPAC). The carefully examined dataset contains data of 85 radiosonde stations, 32 of them in the tropics (Free et al., 2005). The QBO and ENSO signals in the temperature were removed. To calculate the temperature anomalies, the average of the two years before the eruption was subtracted from the average over the two years after the eruption. The corresponding model data of AGUNG1 and AGUNG2 were calculated by averaging over the two

years after the first eruption and subtracting an ensemble mean of control simulations with nudged QBO data, but no volcanic eruption, for the period 1964 to 1965. This provides the anomaly and removes the QBO signal at the same time.

3 Results
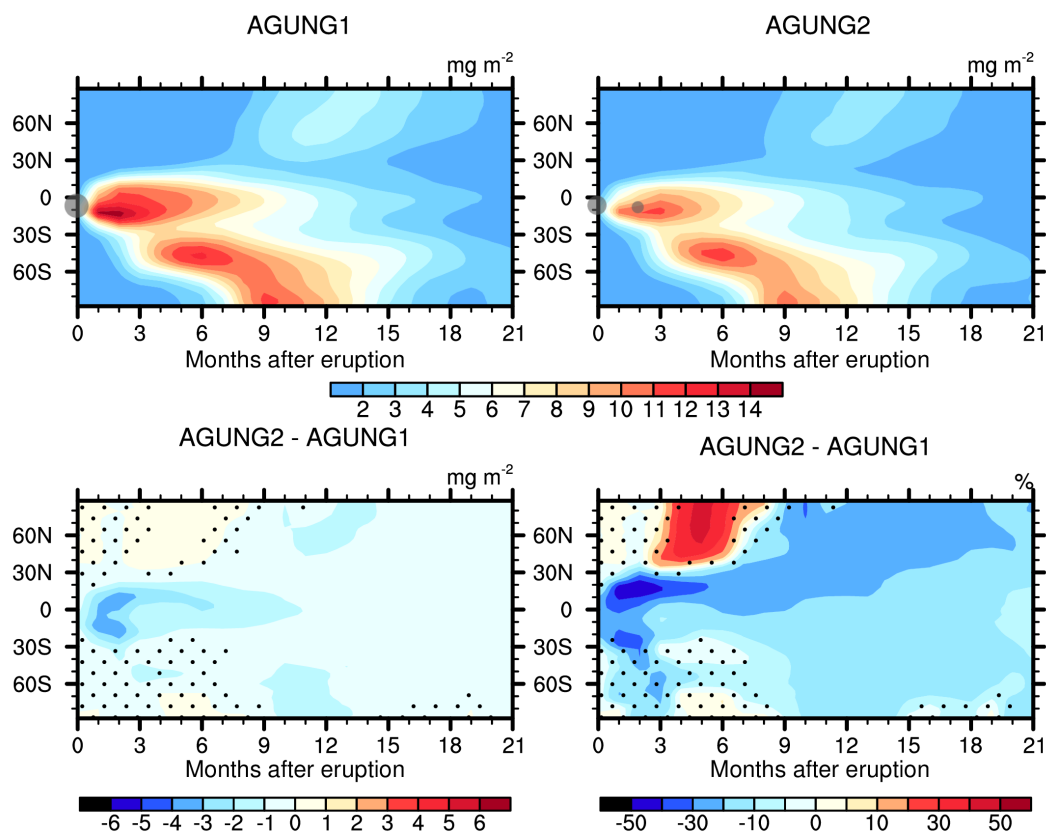
Figure 1. Top: Ensemble mean of sulfate burden of experiments AGUNG1 (left) and AGUNG2 (right). Bottom: Absolute (left) and relative differences (right) of the two ensembles. X-axis gives the months after the first eruption in March 1963. Stippling indicates non-significant differences at 99% level, following a student-t test. The gray dots mark the location and size of the volcanic eruptions.

Figure 1 shows the monthly and zonally averaged sulfate burden of the ensemble mean. Mt. Agung is located at $8°$ in the southern hemisphere (SH) tropics. Thus, the main transport direction of the aerosols is southward and, hence, burden values in

the northern hemisphere (NH) remain small. The ensemble mean shows for both experiments, AGUNG1 and AGUNG2, two areas with high burden: a maximum in the southern tropics in the months 1 to 3 after the eruption, and about four months later in the SH mid- and high-latitudes with a secondary maximum between $30°S$ and $60°S$. The maximum burden is slightly above 14 mg/m^2 in the ensemble of AGUNG1 and 10 mg/m^2, about 30% lower, in the ensemble of AGUNG2, reflecting the ratio of the initial injection. The initially higher injection in the ensemble of AGUNG1 results in a higher burden over almost all simulated months and regions. The strongest absolute difference between the two ensembles occurs in the time period between both climatic eruptions, when the injected sulfur amount in AGUNG2 is still smaller. The relative difference highlights that more aerosols are transported into the NH tropics in AGUNG2 in the first months after the second eruption (months 4 to 6). The burden of AGUNG2 increases slightly after the second eruption but, overall, the tropical maximum of the burden is smaller and occurs later than in AGUNG1. In the SH extratropics the differences between the two ensembles are below 20%, 1 to 2 mg/m^2. In contrast, the burden is up to 50% larger in AGUNG2 in months 6 to 10 in the NH extratropics, poleward of $30°N$, but with small absolute values. Also towards NH winter the relative difference between the two simulations is larger in the NH than in the SH, which indicates differences in the transport regime and wind systems.

3.1 Transport of aerosols

The ensemble of AGUNG2 results in most areas and times in a lower sulfate burden than AGUNG1 (Fig. 1). An exception is the sulfate burden in the extratropics in the first months after the second eruption. This indicates a stronger meridional transport in AGUNG2. The second eruption occurs two months later, thus, in a different season with different stratospheric transport pattern. Additionally, the injection altitude is lower, 70 hPa instead of 50 hPa. Figure 2 shows the monthly mean zonal wind (shaded) and the residual stream function for April and June 1963, one month after the eruption each, of AGUNG2 (see Fig. 5 in supplementary material for results of AGUNG1). Nudging of the QBO at the Equator results in similar zonal mean zonal winds in the tropics between the two experiments. Differences of the zonal mean zonal wind in the extratropics, around $\pm 10\%$, are not significant and are mainly caused by a meridional shift of the higher latitude wind systems.

Punge et al. (2009) showed that meridional transport in the tropics and sub-tropics depends on the QBO phase. Figure 2 shows that both eruptions phases inject into easterly zonal wind. Thus, the QBO phase should not play an important role in transport characteristics of both experiments. Seasonality seems more important. The streamlines show that the zero-line, indicating the tropical pipe, is shifted northward in June, allowing more sulfate to be transported into the NH. Additionally, the second eruption occurs at a lower altitude, 70 hPa, where the sub-tropical transport barrier is weaker than at 50 hPa. This allows more meridional transport than at 50 hPa: the stream line at 70 hPa in June is stronger than at 50 hPa in April, 100 kg s^{-1} and around 50 kg s^{-1}, respectively.

3.2 Cumulative impact — a sum over time

The zonally averaged cumulative burden (Fig. 3, left), time integrated monthly mean values over 21 months, starting with the month of the first eruption, is roughly 20% lower for AGUNG2 than AGUNG1. The difference between the two results is larger in the tropics than in the secondary maximum around $50°S$. This results from the stronger meridional transport towards the SH
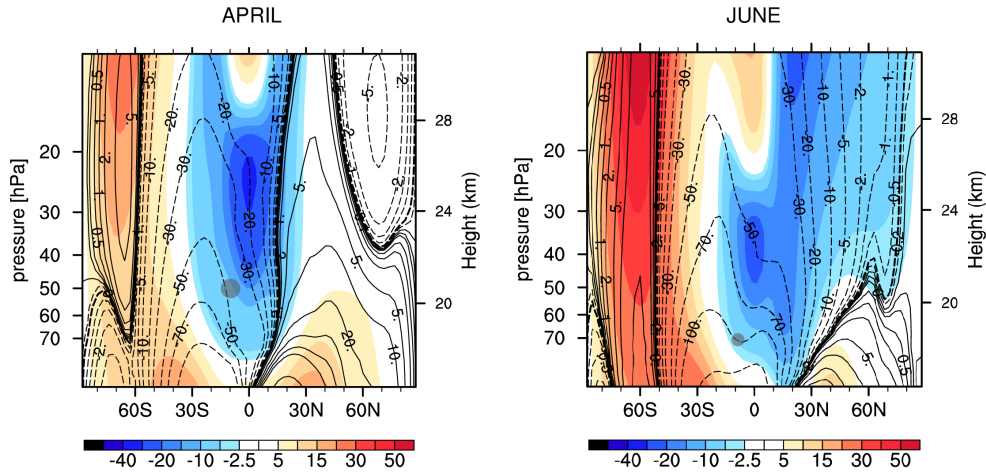
Figure 2. Monthly mean zonal wind $[\mathrm{ms}^{-1}]$ of AGUNG2 for April (left) and June (right) 1963 in shading. Contour lines show the stream function $[\mathrm{kg\,s}^{-1}]$. Positive (solid) streamlines describe clockwise circulation, negative (dashed) ones counter-clockwise circulation. The gray dots mark the injection location of the two volcanic eruptions.

in AGUNG2. Thus, one eruption with larger SO_2 injection results in higher burden than the same injected amount of SO_2, but split into two eruptions and in a slightly stronger tropical confinement of the aerosols. However, the shaded areas indicate that the variance within each ensemble is larger than the differences between the ensemble mean values. This result is confirmed in
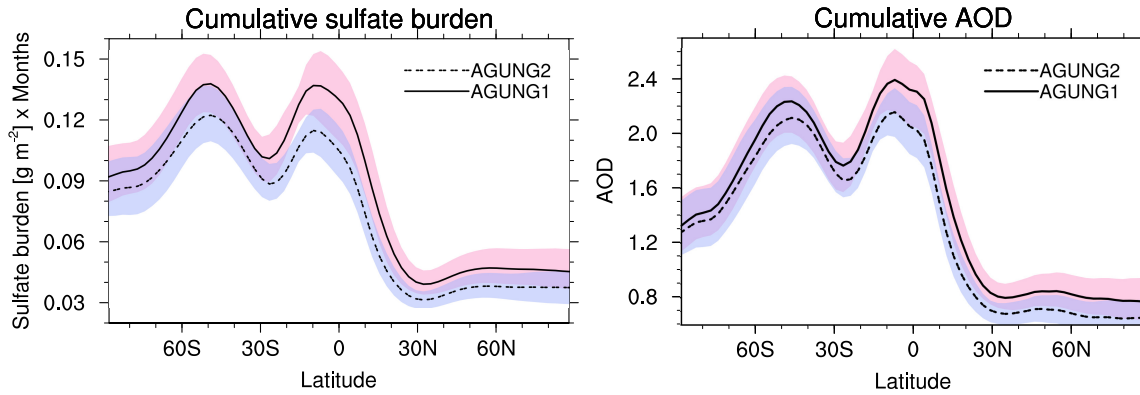
Figure 3. Cumulative values, integral over 21 monthly mean values, of (left) zonally averaged sulfate burden and (right) AOD at 550 nm. The shadings indicate the maximum and minimum values of the single simulations in the ensemble.

the cumulative AOD (Fig. 3, right). But, the AOD of AGUNG1 and AGUNG2 differs less (about 10%) than the burden (about 20%) in the tropics and even less in the SH extra-tropics (about 6%). The reason for this are different particle radii. Scattering

7
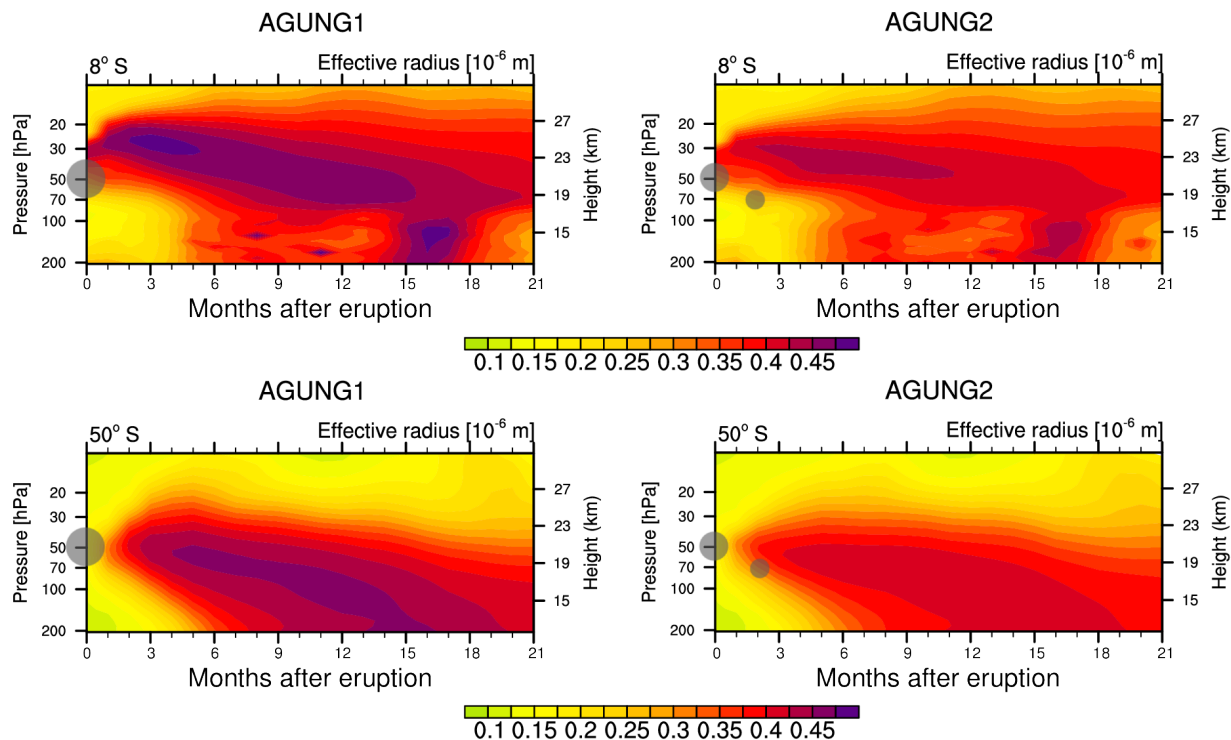
Figure 4. Hovmøller diagram of monthly mean effective radius μm of sulfate at the grid point corresponding to 8°S (top) and 50°S (bottom).

of sulfate aerosols decreases with increasing particle radius. The maximum effective radii of the sulfate aerosols reach 0.5 μm at 8°S for AGUNG1 and stay below 0.45 μm for AGUNG2 (Figure 4, top). Sulfate particles are 0.05 μm smaller in AGUNG2. Thus, they scatter more intensely and the AOD difference between the two experiments gets smaller. These smaller radii are the consequence of the lower injection rate of the first eruption in AGUNG2. Particle sizes increase with increasing injection rate

5 (Niemeier and Timmreck, 2015). Laakso et al. (2016) simulated an volcanic eruption into background sulfate level and into elevated sulfate level from continuous injections for climate engineering (CE). They show a shorter lifetime and larger particles under CE conditions. Thus, following Laakso et al. (2016), we would expect stronger coagulation after the second eruption, as newly formed particles coagulate fast with available larger particles. But the second eruption occurs at lower altitude, where sulfate concentration and particle radii are smaller. Thus, coagulation is less important. We performed an additional sensitivity

10 study where we injected the SO_2 in both eruptions at 50 hPa to differentiate better between injection rates and emission height. The sensitivity simulation AGUNG2-50hPa, with both eruptions at the same altitude, results in particle radii very similar to AGUNG1 and about 0.05 μm larger than in AGUNG2. This reflects the results of Laakso et al. (2016). See Section 2 in supplementary material for more information and figures.
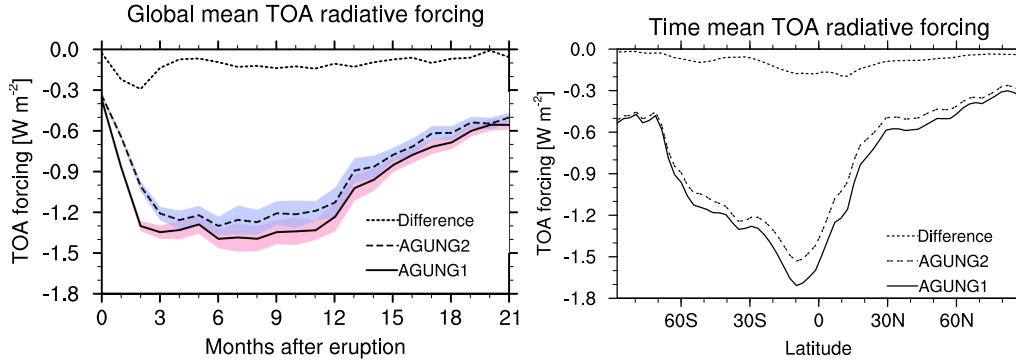
Figure 5. Top of the atmosphere (TOA) radiative forcing of sulfate aerosols under all sky conditions. Aerosol forcing was calculated using a radiation double call. Left: Global mean TOA forcing over time. The shadings indicate the 2σ variability range for both ensembles. Right: Zonally averaged radiative forcing as average over time (21 months).

The climatic impact can be derived from the aerosol radiative forcing at top of the atmosphere (TOA), which was calculated with a radiation double call (Figure 5, left). The spread of the single ensemble members is large, but the average of the AGUNG2 ensemble is just out of the 2σ ensemble variability of AGUNG1. The global monthly mean TOA forcing of sulfate is about 0.1 to 0.3 $\mathrm{Wm^{-2}}$ larger in AGUNG1. The average difference in the short-term volcanic forcing over the 1st 21 post eruption months is three to ten times larger than the long-term forcing radiative forcing of stratospheric ozone (-0.033 $\mathrm{Wm^{-2}}$) in CMIP6 (Checa-Garcia et al., 2018) and comparable to the long-term radiative forcing of the total ozone column (0.28 $\mathrm{Wm^{-2}}$ in CMIP6). The long-term radiative forcing of anthropogenic sulfate aerosols is assumed as -0.4 $\mathrm{Wm^{-2}}$ (Stocker et al., 2013).

We estimate surface temperature changes (ΔT_s) to give a rough estimate of the consequences of this forcing differences. ΔT_s relates to forcing as $\Delta T_s = \alpha F$, with F the radiative forcing and α the climate sensitivity (Gregory and Webb, 2008; Ramaswamy et al., 2001). α is a constant which differs for each model. Thus in our case

$$\frac{\Delta T_s(AGUNG1)}{\Delta T_s(AGUNG2)} = \frac{F(AGUNG1)}{F(AGUNG2)} = \frac{-1.35\mathrm{Wm^{-2}}}{-1.23\mathrm{Wm^{-2}}} = 1.1, \tag{1}$$

with F(AGUNG1) and F(AGUNG2) the averages over the global radiative forcing of the months 3 to 9 after the eruption (Figure 5, left). Thus, we overestimate the surface cooling in AGUNG1 by a factor of 1.1 or 10%. Both experiments show the strongest difference of radiative forcing in the tropics (Figure 5, right) and the strongest surface cooling occurs in the tropics as well.

4 Comparison to observations

The zonally averaged AOD of AGUNG1 and AGUNG2 differs mainly in the tropics (Figure 6, top) and is rather similar in the SH extratropics. Our results agree quite well to the CMIP6 AOD, which shows, however, slower transport into the extra-tropics and no secondary maximum at 40°S to 50°S. Less aerosols reach the SH high-latitudes in CMIP6, but they have a longer lifetime. The CMIP5 volcanic forcing data used for the MPI-ESM simulations show a very different evolution which might be related to not reliable measurements in the tropics (Stothers, 2001).
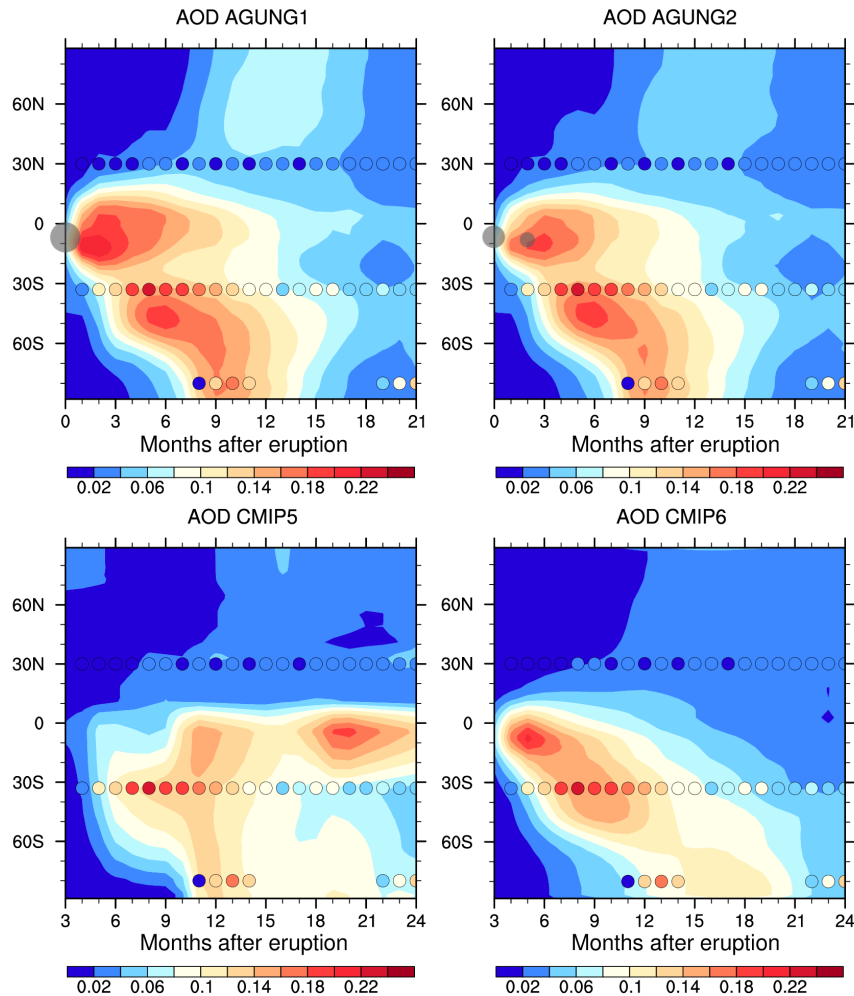
Figure 6. Monthly mean AOD at 550 μm over time. Top: AGUNG1 and AGUNG2 ensemble. Bottom: AOD used for CMIP5 simulations (Stenchikov et al., 1998) and AOD for CMIP6 simulations Luo (2016). Overlayed as colored circles are measurements of monthly mean AOD averaged over the regions 20°N to 40°N and 20°S to 40°S, given in Table 3 of Stothers (2001), and single values for the South pole (after Figure 2, same paper). The gray circles mark the volcanic eruptions, the size represents the size of the eruption.

Both AGUNG experiments fit in general well to the measurements of Stothers (2001), which are included as circles in Figure 6. The simulated NH AOD is slightly larger than the measurements. Thus, it seems that ECHAM-HAM overestimates the northward transport, but we have to take into account that Stothers (2001) noted the measured NH AOD is barely above noise level. In the SH the modeled AOD is smaller than the measurements, but larger than the CMIP6 data. In ECHAM-HAM,

5   meridional exchange within the sub-tropics results in lower values between 20°S and 30°S and a maximum at 50°S where the meridional transport is blocked by the edge of the polar vortex. This maximum AOD, above 0.2, is more similar to the measured AOD between 20°S and 40°S which could be an indication for too strong meridional transport in ECHAM-HAM. The AOD measurements of the months 19 to 21 and the CMIP6 data may indicate a too short lifetime of the simulated aerosols at the SH high latitudes. This is most probably related to too intense sedimentation at high latitudes (Brühl et al., 2018) in the T42

10   resolution of ECHAM5. The consequence is too high wet deposition at high latitudes, a well known phenomena phenomena of ECHAM-HAM.
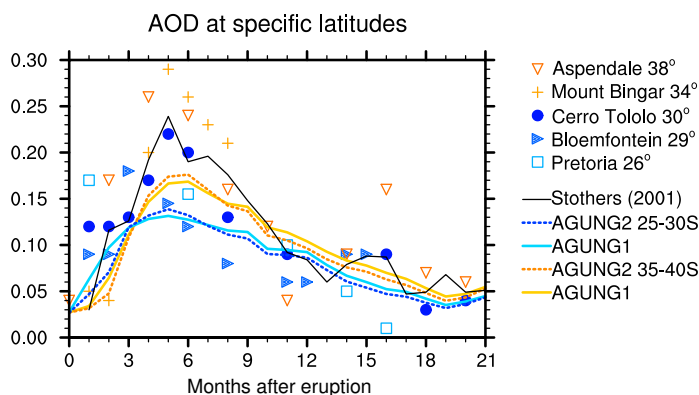

Figure 7. Monthly mean SH AOD (550 μm) over time. Colored lines show model results averaged over 25°S to 30°S (blue) and 35°S to 40°S (orange), each for both ensembles. The black line gives data of Stothers (2001), average of measurements between 20°S and 40°S. Single markers show single measurement data, estimated from Figure 1 in Stothers (2001), with a similar color code than the model data.

A more detailed analyses of the SH extra-tropics is shown in Figure 7. We averaged the model data over latitude bands 25°S to 30°S and 35°S to 40°S to compare those to the single measurement data given in Figure 1 of Stothers (2001). The simulated AOD is clearly smaller than the point measurements, but one should take into account that horizontal gradients in a volcanic cloud can be large. Thus, a point measurement should give a higher value than an area mean of a model, which represents an

15   area of several hundred kilometers. Additionally, measurements and simulated values depend not only on sulfate evolution but also on transport. Further possible reasons for the differences were stated before. In the first three months after the eruption, the simulated AOD agrees well to the measurements. The onset of the meridional transport is similar, but the simulated volcanic cloud arrives slightly later in 25°S to 30°S (see also Fig 6). The agreement between the model simulations and the individual

11

stations differ with time. Between 35°S to 40°S, the model agrees better with the data of Mt. Bingar (yellow cross) than to the Aspendale data (red triangle) in the first months after the eruption, where the sulfate values increase two months earlier although the station is closer to the tropics. This may indicate the dependency of the point source to the position of the volcanic cloud. Both, the timing of the maximum and the onset of the decline agree well in measurements and model results.

5   Measured data of particle radii are not available, but the following references provide some estimates, which are helpful for a rough comparison. Arfeuille et al. (2014) simulated for the SAGE-4λ dataset effective radii of 0.3 µm to 0.4 µm for eruptions of the size of the the Agung eruption. Stothers (2001) estimates a radius of 0.35 µm from the measurement data of the year 1963 at Bloemfontain, South Africa (29°S). Our simulated radii at the Equator (above 0.45 µm) and at 50°S (above 0.4 µm) are larger than these values for both experiments (Figure 4), with a better agreement in AGUNG2. A smaller radius of the
10   aerosols would cause a larger AOD. The larger radii in our experiments lead us to the question of the requirement to include an OH-limitation process for modeling the sulfate evolution, which is a still open research question. In case of high SO_2 concentrations OH might be limited for further SO_2 oxidation (Bekki et al., 1996). The slower formation of sulfuric acid vapor would result in smaller particles. Bekki et al. (1996) assumed that OH limitation occurs only in case of a super-eruption, but Mills et al. (2017) show OH-limitation also after the Mt. Pinatubo eruption. On the other hand, LeGrande et al. (2016) showed
15   that water vapor in the eruption cloud increases the amount of available OH. This reaction was not included in the two studies cited above. The results presented here use a fixed monthly mean OH concentration which is not influenced by the volcanic cloud. Following Mills et al. (2017), this missing OH limitation leads to faster formation of sulfate resulting in larger sulfate particles. Therefore, we performed one simulation with a simple parameterization of OH limitation, see the supplementary materials for details. This simulation shows slower sulfate formation, which agrees less with the measurements, and only a
20   slightly higher AOD half a year after the eruption (Figure 4 and Figure 5 in supplementary materials) for the OH-limited case. As we use a simplistic parameterization these results are very limited.

    Sulfate aerosol absorbs terrestrial radiation and warms the stratosphere. This temperature signal depends in the model on the coupling to radiation. We compare the results of the ensemble mean temperature data to radiosonde data of Free and Lanzante (2009). Both, model and measurement data are independent of QBO temperature relations (see Section 2.3). The measurements,
25   averaged over stations between 30°N and 30°S, show a strong maximum at 70 hPa (Figure 8). The average over 30°N to 30°S of the model results (black lines) show a smaller anomaly and a stronger vertical extension of the heated area, more in AGUNG1 than in AGUNG2. Below the maximum at 70 hPa the simulated temperature than the measurements. Both features indicate too strong vertical lofting in the model. Figures 6 and 7 indicated a too low AOD in the model results around 30°S. Therefore, we added a second temperature profile, averaged over the main volcanic cloud at 15°N to 15°S (gray line), to Figure 8. Now
30   the maximum is represented better. More important is the better agreement with the temperature decrease between 50 hPa and 70 hPa, especially for AGUNG2. The easterly phase of the QBO is related to downward motion and suppresses the vertical lofting caused by the heating, but is also also related to stronger vertical transport in the secondary meridional circulation around 30°North and South. This up welling seems to be stronger in the model than in the measurements causing the too high vertical extension of the simulated cloud. While theses results compare well to the radiosonde data, simulated temperature
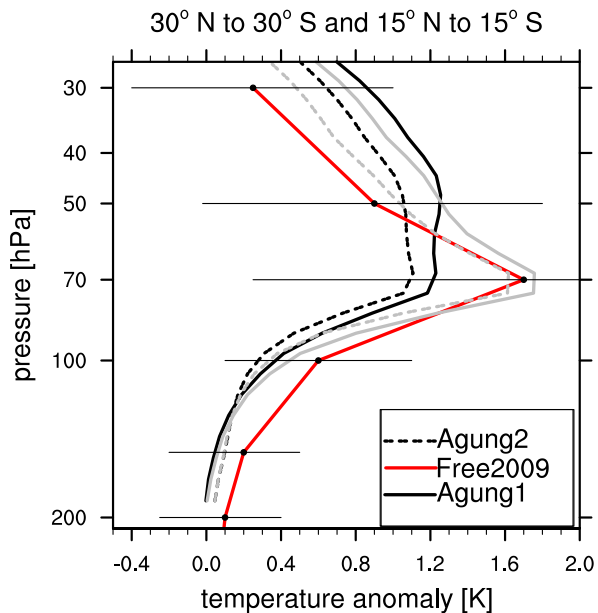
Figure 8. Profile of temperature anomaly [K] compared to RATPAC radiosonde measurements taken from (Free and Lanzante, 2009) in the tropics (30°N to 30°S): Results averaged over 30°N to 30°S (black) and results averaged over 15°N to 15°S (gray)). Model results and measurements are averaged over two years after the eruption. The horizontal lines mark the 95% confidence interval for the RATPAC observations.

anomalies are only half of the observed one in the SH (not shown). This may hint towards a too short lifetime of the simulated sulfate aerosols (see Figure 6 too).

5 Summary and conclusions

We compared results of two scenarios for the Mt. Agung eruption in 1963: the commonly used one eruption scenario with a strength of 7 Tg SO_2 and compared this to a scenario with two eruptions. From AOD measurements one single number of the injected sulfur amount was estimated, but observation and detection of the mass flux show a scenario of two eruptions. Therefore, we assumed a scenario with two climatic eruptions of 4.7 Tg SO_2 and 2.3 Tg SO_2 respectively. We simulated a lower burden in the tropics, but slightly stronger meridional flow into the extratropics in the simulation with two eruptions, AGUNG2. We relate the stronger meridional flow to the lower injection altitude of the second eruption, where the tropical transport barrier is weaker. Additionally, the position of the tropical pipe is further northward in May than in March. This allows more aerosols to be transported into the NH. The smaller injection rate and the two different injection altitudes cause the particle to grow less than in AGUNG1. These processes result in 10% to 20% lower radiative forcing, or 0.1 to 0.3 Wm^{-2}

in monthly mean global average, and estimated 10% less surface cooling in AGUNG2. The strongest signal would occur in the tropics.

When comparing to the few available measurements we see that the differences to the measurements are larger than the differences between the two experiments. We seem to underestimate the observed AOD and simulate larger particle radii. The timing of the aerosol evolution in the model seems to be supported by the measurements. Given the low number of observations at that time, especially in the tropics, it is difficult to validate the two experiments. Overall, the smaller particle size and slightly better shape of the temperature anomaly in the vertical profile of AGUNG2 are consequences of different transport and microphysical processes between the two experiments. These are arguments to include both climatic eruptions into future emission datasets.

One could also argue that the large model spread, as e.g. described by Marshall et al. (2018) and Zanchettin et al. (2016), limits the interpretation of our model results. Other models may get quantitatively different results, but most probably the simulated difference between the two eruption scenarios would be qualitatively similar: A lower radiative forcing of the Agung 1963 eruption when including two eruption phases. Including a more sophisticated atmospheric chemistry (including OH chemistry, water vapor and ozone) may increase the differences between the scenarios. Lower SO_2 injection rates in AGUNG2 would cause less impact on OH and ozone, thus on chemical species in the stratosphere. Taking two eruptions phases into account will be important for processes in the early evolution of sulfate. Ash and ice are important species in this early phase. Both were not taken into account in the here presented simulations but are planed for the future.

Overall, differences of around 10% in the radiative forcing between AGUNG1 and AGUNG2 should justify changes in the volcanic emission datasets. The more recent volcano datasets are rather detailed. Also future studies using high horizontal and vertical resolution and more sophisticated models will demand detailed input data. Details of our assumptions on the Agung eruptions might be critically reviewed again but, we recommend to include both eruptions of Mt. Agung in upcoming datasets.

References

Ammann, C. M., Meehl, G. A., Washington, W. M., and Zender, C. S.: A monthly and latitudinally varying volcanic forcing dataset in simulations of 20th century climate, GRL, 30, 1657, https://doi.org/10.1029/2003GL016875, 2003.

Aquila, V., Garfinkel, C. I., Newman, P., Oman, L. D., and Waugh, D. W.: Modifications of the quasi-biennial oscillation by a geoengineering perturbation of the stratospheric aerosol layer, Geophys. Res. Lett., 41, 1738–1744, https://doi.org/10.1002/2013GL058818, 2014.

Arfeuille, F., Weisenstein, D., Mack, H., Rozanov, E., Peter, T., and Brönnimann, S.: Volcanic forcing for climate modeling: a new microphysics-based data set covering years 1600–present, Climate of the Past, 10, 359–375, https://doi.org/10.5194/cp-10-359-2014, https://www.clim-past.net/10/359/2014/, 2014.

Bekki, S., Pyle, J. A., Zhong, W., Haigh, R. T. J. D., and Pyle, D. M.: The role of microphysical and chemical processes in prolonging the climate forcing of the Toba eruption, Geophys. Res. Lett., 23, 2669–2672, 1996.

Brühl, C., Schallock, J., Klingmüller, K., Robert, C., Bingen, C., Clarisse, L., Heckel, A., North, P., and Rieger, L.: Stratospheric aerosol radiative forcing simulated by the chemistry climate model EMAC using Aerosol CCI satellite data, Atmospheric Chemistry and Physics, 18, 12 845–12 857, https://doi.org/10.5194/acp-18-12845-2018, 2018.

CCMVal, S.: SPARC Report on the Evaluation of Chemistry-Climate Models, https://doi.org/http://www.atmosp.physics.utoronto.ca/SPARC, sPARC Report No. 5, WCRP-132, WMO/TD-No. 1526, V. Eyring, T. G. Shepherd, D. W. Waugh (Eds.), 2010.

Checa-Garcia, R., Hegglin, M. I., Kinnison, D., Plummer, D. A., and Shine, K. P.: Historical Tropospheric and Stratospheric Ozone Radiative Forcing Using the CMIP6 Database, Geophysical Research Letters, 45, 3264–3273, https://doi.org/10.1002/2017GL076770, https://agupubs.onlinelibrary.wiley.com/doi/abs/10.1002/2017GL076770, 2018.

Crowley, T., Zielinski, G., Vinther, B., Udisti, R., Kreutz, K., Cole-Dai, J., and Castellano, E.: Volcanism and the little ice age, PAGES News, 16, 22–23, 2008.

Crowley, T. J. and Unterman, M. B.: Technical details concerning development of a 1200-yr proxy index for global volcanism, Earth System Science Data Discussions, 5, 1–28, https://doi.org/10.5194/essdd-5-1-2012, 2012.

Dyer, A. J. and Hicks, B. B.: Global spread of volcanic dust from the Bali eruption of 1963, Quarterly Journal of the Royal Meteorological Society, 94, 545–554, https://doi.org/10.1002/qj.49709440209, https://rmets.onlinelibrary.wiley.com/doi/abs/10.1002/qj.49709440209, 1968.

Fontijn, K., Costa, F., Sutawidjaja, I., Newhall, C. G., and Herrin, J. S.: A 5000-year record of multiple highly explosive mafic eruptions from Gunung Agung (Bali, Indonesia): implications for eruption frequency and volcanic hazards, Bulletin of Volcanology, 77, 59, https://doi.org/10.1007/s00445-015-0943-x, https://doi.org/10.1007/s00445-015-0943-x, 2015.

Free, M. and Lanzante, J.: Effect of volcanic eruptions on the verti- cal temperature profile in radiosonde data and climate models, J. Climate, 22, 2925–2939, https://doi.org/https://doi.org/10.1175/2008JCLI2562.1, 2009.

Free, M., Seidel, D. J., Angell, J. K., Lanzante, J., Durre, I., and Peterson, T. C.: Radiosonde Atmospheric Temperature Products for Assessing Climate (RATPAC): A new data set of large-area anomaly time series, Journal of Geophysical Research: Atmospheres, 110, https://doi.org/10.1029/2005JD006169, https://agupubs.onlinelibrary.wiley.com/doi/abs/10.1029/2005JD006169, 2005.

Gao, C., Robock, A., and Ammann, C.: Volcanic forcing of climate over the past 1500 years: An improved ice core-based index for climate models, Journal of Geophysical Research: Atmospheres, 113, https://doi.org/10.1029/2008JD010239, https://agupubs.onlinelibrary.wiley.com/doi/abs/10.1029/2008JD010239, 2008.

Gertisser, R., Deegan, F., Troll, V., and Preece, K.: When the gods are angry: volcanic crisis and eruption at Bali's great volcano, Geology Today, 34, 62–65, https://doi.org/10.1111/gto.12224, https://onlinelibrary.wiley.com/doi/abs/10.1111/gto.12224, 2018.

Giorgetta, M. A. and Bengtsson, L.: Potential role of the quasi–biennial oscillation in the stratosphere–troposphere exchange as found in water vapor in general circulation model experiments, J. Geophys. Res., 104, 6003–6019, 1999.

Giorgetta, M. A., Manzini, E., Roeckner, E., Esch, M., and Bengtsson, L.: Climatology and forcing of the quasi–biennial oscillation in the MAECHAM5 model, J. Climate, 19, 3882–3901, 2006.

Gregory, J. and Webb, M.: Tropospheric adjustment induces a cloud component in CO_2 forcing, J. Climate, 21, 58–71, https://doi.org/10.1175/2007JCLI1834.1, 2008.

Hansen, J. E., Wang, W.-C., and Lacis, A. A.: Mount Agung Eruption Provides Test of a Global Climatic Perturbation, Science, 199, 1065–1068, https://doi.org/10.1126/science.199.4333.1065, http://science.sciencemag.org/content/199/4333/1065, 1978.

Hansen, K.: NASA Earth Observatory: Tracking the Sulfur Dioxide from Mount Agung, https://earthobservatory.nasa.gov/images/91329/tracking-the-sulfur-dioxide-from-mount-agung, last access: February 28, 2019, 2017.

Hommel, R., Timmreck, C., and Graf, H. F.: The global middle-atmosphere aerosol model MAECHAM5-SAM2: comparison with satellite and in-situ observations, Geoscientific Model Development, 4, 809–834, https://doi.org/10.5194/gmd-4-809-2011, http://www.geosci-model-dev.net/4/809/2011/, 2011.

Hurrell, J. W., Hack, J. J., Shea, D., Caron, J. M., and Rosinski, J.: A New Sea Surface Temperature and Sea Ice Boundary Dataset for the Community Atmosphere Model, Journal of Climate, 21, 5145–5153, https://doi.org/10.1175/2008JCLI2292.1, https://doi.org/10.1175/2008JCLI2292.1, 2008.

Laakso, A., Kokkola, H., Partanen, A.-I., Niemeier, U., Timmreck, C., Lehtinen, K. E. J., Hakkarainen, H., and Korhonen, H.: Radiative and climate impacts of a large volcanic eruption during stratospheric sulfur geoengineering, Atmospheric Chemistry and Physics, 16, 305–323, https://doi.org/10.5194/acp-16-305-2016, https://www.atmos-chem-phys.net/16/305/2016/, 2016.

LeGrande, A. N., Tsigaridis, K., and Bauer, S.: Role of atmospheric chemistry in the climate impacts of stratospheric volcanic injections, Nature Geoscience, 9, 653, https://doi.org/10.1038/ngeo2771, 2016.

Luo, B.: Stratospheric aerosol data for use in CMIP6 models – data description, ftp://iacftp.ethz.ch/pub_read/luo/CMIP6/Readme_Data_Description.pdf, version January, 8th 2019, 2016.

Marchese, F., Falconieri, A., Pergola, N., and Tramutoli, V.: Monitoring the Agung (Indonesia) Ash Plume of November 2017 by Means of Infrared Himawari 8 Data, Remote Sensing, 10, https://doi.org/10.3390/rs10060919, http://www.mdpi.com/2072-4292/10/6/919, 2018.

Marshall, L., Schmidt, A., Toohey, M., Carslaw, K. S., Mann, G. W., Sigl, M., Khodri, M., Timmreck, C., Zanchettin, D., Ball, W. T., Bekki, S., Brooke, J. S. A., Dhomse, S., Johnson, C., Lamarque, J.-F., LeGrande, A. N., Mills, M. J., Niemeier, U., Pope, J. O., Poulain, V., Robock, A., Rozanov, E., Stenke, A., Sukhodolov, T., Tilmes, S., Tsigaridis, K., and Tummon, F.: Multi-model comparison of the volcanic sulfate deposition from the 1815 eruption of Mt. Tambora, Atmospheric Chemistry and Physics, 18, 2307–2328, https://doi.org/10.5194/acp-18-2307-2018, https://www.atmos-chem-phys.net/18/2307/2018/, 2018.

Mills, M. J., Richter, J. H., Tilmes, S., Kravitz, B., MacMartin, D. G., Glanville, A. A., Tribbia, J. J., Lamarque, J.-F., Vitt, F., Schmidt, A., Gettelman, A., Hannay, C., Bacmeister, J. T., and Kinnison, D. E.: Radiative and Chemical Response to Interactive Stratospheric Sulfate Aerosols in Fully Coupled CESM1(WACCM), Journal of Geophysical Research: Atmospheres, 122, 13,061–13,078, https://doi.org/10.1002/2017JD027006, http://dx.doi.org/10.1002/2017JD027006, 2017JD027006, 2017.

Naujokat, B.: An update of the observed quasi–biennial oscillation of the stratospheric winds over the tropics, J. Atmos. Sci., 43, 1873–1877, 1986.

17

Neely III, R. and Schmidt, A.: VolcanEESM: Global volcanic sulphur dioxide (SO2) emissions database from 1850 to present - Version 1.0., https://doi.org/10.5285/76ebdc0b-0eed-4f70-b89e-55e606bcd568, http://dx.doi.org/10.5285/76ebdc0b-0eed-4f70-b89e-55e606bcd568, centre for Environmental Data Analysis, 2016.

Niemeier, U. and Schmidt, H.: Changing transport processes in the stratosphere by radiative heating of sulfate aerosols, Atmospheric Chemistry and Physics, 17, 14 871–14 886, https://doi.org/10.5194/acp-17-14871-2017, https://www.atmos-chem-phys.net/17/14871/2017/, 2017.

Niemeier, U. and Timmreck, C.: What is the limit of climate engineering by stratospheric injection of SO2?, Atmospheric Chemistry and Physics, 15, 9129–9141, https://doi.org/10.5194/acp-15-9129-2015, http://www.atmos-chem-phys.net/15/9129/2015/, 2015.

Niemeier, U., Timmreck, C., Graf, H.-F., Kinne, S., Rast, S., and Self, S.: Initial fate of fine ash and sulfur from large volcanic eruptions, Atmospheric Chemistry and Physics, 9, 9043–9057, http://www.atmos-chem-phys.net/9/9043/2009/, 2009.

Punge, H. J., Konopka, P., Giorgetta, M. A., and Müller, R.: Effects of the quasi-biennial oscillation on low-latitude transport in the stratosphere derived from trajectory calculations, J. Geophys. Res., 114, D03 102, https://doi.org/10.1029/2008JD010518, 2009.

Ramaswamy, V., Boucher, O., Haigh, J., Hauglustaine, D., Haywood, J., Myhre, G., Nakajima, T., Shi, G., and Solomon, S.: Radiative Forcing of Climate Change, in: Climate Change 2001: The Scientific Basis. Contribution of Working Group I to the Third Assessment Report of the Intergovernmental Panel on Climate Change, edited by Houghton, J., Ding, Y., Griggs, D., M. Noguer, P. v. d. L., Dai, X., Maskell, K., and Johnson, C., chap. 6, p. 881pp, Cambridge University Press, Cambridge, United Kingdom and New York, NY, USA, 2001.

Revell, L. E., Stenke, A., Luo, B., Kremser, S., Rozanov, E., Sukhodolov, T., and Peter, T.: Impacts of Mt Pinatubo volcanic aerosol on the tropical stratosphere in chemistry-climate model simulations using CCMI and CMIP6 stratospheric aerosol data, Atmospheric Chemistry and Physics, 17, 13 139–13 150, https://doi.org/10.5194/acp-17-13139-2017, 2017.

Sato, M., Hansen, J. E., McCormick, M. P., and Pollack, J. B.: Stratospheric aerosol optical depths, JGR, 98, 22 987, https://doi.org/doi.wiley.com/10.1029/93JD02553, 1993.

Self, S. and King, A. J.: Petrology and sulfur and chlorine emissions of the 1963 eruption of Gunung Agung, Bali, Indonesia, Bulletin of Volcanology, 58, 263–285, https://doi.org/10.1007/s004450050139, 1996.

Self, S. and Rampino, M. R.: The 1963–1964 eruption of Agung volcano (Bali, Indonesia), Bulletin of Volcanology, 74, 1521–1536, https://doi.org/10.1007/s00445-012-0615-z, 2012.

Stenchikov, G. L., Kirchner, I., Robock, A., Graf, H.-F., Antuña, J. C., Grainger, R. G., Lambert, A., and Thomason, L.: Radiative forcing from the 1991 Mount Pinatubo volcanic eruption, J. Geophys. Res., 103, 13 837–13 858, 1998.

Stier, P., Feichter, J., Kinne, S., Kloster, S., Vignati, E., Wilson, J., Ganzeveld, L., Tegen, I., Werner, M., Balkanski, Y., Schulz, M., Boucher, O., Minikin, A., and Petzold, A.: The aerosol–climate model ECHAM5–HAM, Atmos. Chem. Phys., 5, 1125–1156, 2005.

Stocker, T. F., Dahe, Q., and Plattner, G.-K.: Climate Change 2013: The Physical Science Basis, Working Group I Contribution to the Fifth Assessment Report of the Intergovernmental Panel on Climate Change. Summary for Policymakers (IPCC, 2013), 2013.

Stothers, R. B.: Major optical depth perturbations to the stratosphere from volcanic eruptions: Stellar extinction period, 1961–1978, Journal of Geophysical Research: Atmospheres, 106, 2993–3003, https://doi.org/10.1029/2000JD900652, 2001.

Timmreck, C.: Three–dimensional simulation of stratospheric background aerosol: First results of a multiannual general circulation model simulation, J. Geophys. Res., 106, 28 313–28 332, 2001.

Timmreck, C., Graf, H.-F., Lorenz, S. J., Niemeier, U., Zanchettin, D., Matei, D., Jungclaus, J. H., and Crowley, T. J.: Aerosol size confines climate response to volcanic super-eruptions, Geophys. Res. Lett., 37, L2470, https://doi.org/10.1029/2010GL045464, 2010.

Toohey, M. and Sigl, M.: Volcanic stratospheric sulfur injections and aerosol optical depth from 500 BCE to 1900 CE, Earth System Science Data, 9, 809–831, https://doi.org/10.5194/essd-9-809-2017, https://www.earth-syst-sci-data.net/9/809/2017/, 2017.

Toohey, M., Krüger, K., and Timmreck, C.: Volcanic sulfate deposition to Greenland and Antarctica: A modeling sensitivity study, Journal of Geophysical Research: Atmospheres, 118, 4788–4800, https://doi.org/10.1002/jgrd.50428, https://agupubs.onlinelibrary.wiley.com/doi/abs/10.1002/jgrd.50428, 2013.

Toohey, M., Stevens, B., Schmidt, H., and Timmreck, C.: Easy Volcanic Aerosol (EVA v1.0): an idealized forcing generator for climate simulations, Geoscientific Model Development, 9, 4049–4070, https://doi.org/10.5194/gmd-9-4049-2016, https://www.geosci-model-dev.net/9/4049/2016/, 2016.

Zanchettin, D., Khodri, M., Timmreck, C., Toohey, M., Schmidt, A., Gerber, E. P., Hegerl, G., Robock, A., Pausata, F. S. R., Ball, W. T., Bauer, S. E., Bekki, S., Dho mse, S. S., LeGrande, A. N., Mann, G. W., Marshall, L., Mills, M., Marchand, M., Niemeie r, U., Poulain, V., Rozanov, E., Rubino, A., Stenke, A., Tsigaridis, K., and Tummon, F.: The Model Intercomparison Project on the climatic response to Volcanic forcing (VolMIP): experimental design and forcing input data for CMIP6, Geoscientific Model Development, 9, 2701–2719, https://doi.org/10.5194/gmd-9-2701-2016, https://www.geosci-model-dev.net/9/2701/2016/, 2016.